



## ISTITUTO NAZIONALE DI RICERCA METROLOGICA Repository Istituzionale

Asymmetric CapMix Device Exploiting Functionalized Graphene Oxide and SPEEK Coatings for Improved Energy Harvesting From Salinity Gradients

*Original*

Asymmetric CapMix Device Exploiting Functionalized Graphene Oxide and SPEEK Coatings for Improved Energy Harvesting From Salinity Gradients / Pedico, A.; Molino, D.; Zaccagnini, P.; Bocchini, S.; Bertana, V.; Lamberti, A.. - In: ADVANCED SUSTAINABLE SYSTEMS. - ISSN 2366-7486. - 8:10(2024).  
[10.1002/adsu.202400106]

*Availability:*

This version is available at: 11696/82781 since: 2025-01-10T15:34:16Z

*Publisher:*

John Wiley and Sons Inc

*Published*

DOI:10.1002/adsu.202400106

*Terms of use:*

This article is made available under terms and conditions as specified in the corresponding bibliographic description in the repository

*Publisher copyright*

(Article begins on next page)

# Asymmetric CapMix Device Exploiting Functionalized Graphene Oxide and SPEEK Coatings for Improved Energy Harvesting From Salinity Gradients

Alessandro Pedico,\* Davide Molino, Pietro Zaccagnini, Sergio Bocchini, Valentina Bertana, and Andrea Lamberti

This work investigated the possibility of using functionalized graphene oxide and sulfonated poly(ether ether ketone) coatings on activated carbons to obtain an asymmetric device suitable for Capacitive Mixing (CapMix) application. Herein the synthesis and fabrication procedures of both materials and electrodes are reported, together with a comprehensive list of electrochemical characterization techniques. The results from the electrochemical characterization are used to design the optimal operational parameters for CapMix experiments involving the materials being studied. A homemade cell is designed and fabricated for CapMix application by polymer micromachining. Electrochemical tests are conducted to optimize the process parameters and the results of this optimization are reported, proving that both the materials and the process parameters play a key role in CapMix. The final device can generate a net power output of  $12 \text{ mW m}^{-2}$  by mixing simulated seawater and freshwater. This result paved the way for further application of graphene oxide in the field of renewable energy.

economically. Climate change is a global reminder to do this process following the green path. This must be done by harvesting energy from renewable sources. In the last decades, efforts have been spent trying to harvest energy from salinity gradients.<sup>[1–3]</sup> Indeed, a large amount of energy is dissipated in the form of heat where freshwater meets seawater. Considering all the rivers on Earth, the amount of power at stake is of the order of  $1 \text{ TW}$ .<sup>[4]</sup>

This mixing energy can be harvested using different techniques, able to convert this energy into mechanical or electrical energy. The most famous techniques are Pressure Retarded Osmosis and Reverse Electrodialysis. Both of them rely on membranes to control the mixing of the solutions and to convert the mixing

## 1. Introduction

The energy demand is worldwide continuously increasing. Human settlements, facilities, and electrified mobility put a challenge to engineers and material scientists to provide new materials and technologies to produce energy more efficiently and

energy into electrical power. Among the techniques suited to harvest this energy, Capacitive Mixing is the most recent technique, which combines the supercapacitor technology with a controlled mixing of two solutions to harvest energy in the form of electricity. The working principle hinges on a supercapacitor cell, composed of two porous electrodes, designed in such a way that an electrolyte solution can be flushed between these electrodes.

To harvest energy through the CapMix, a cycle made of four steps is required. In the first step, in open circuit conditions, the space between the electrodes is filled with a highly concentrated solution. In the second step, an external power source provides electrical energy to charge the electrodes up to a fixed voltage. In the third step, the external power source is disconnected, and the solution is replaced with a less concentrated solution. In this step, the injection of low-salinity water causes an expansion of the electrical double layer previously formed on the surface of the electrodes. This expansion, located in the diffuse part of the electrical double layer, is responsible for a voltage rise of the cell. In the final step, the device is discharged on a load to harvest the energy obtained from the spontaneous voltage rise, and the process is repeated. This last step is the key point of the process, in which the chemical energy of the mixing process is converted into electrochemical potential and then harvested in the form of electrical energy by means of an external load.

First proposed by Brogioli in 2009,<sup>[5]</sup> this technique was further studied in the past decade to improve its performance.

A. Pedico, D. Molino, P. Zaccagnini, S. Bocchini, V. Bertana, A. Lamberti  
Dipartimento di Scienza Applicata e Tecnologia (DISAT)  
Politecnico di Torino  
Corso Duca degli Abruzzi, 24, Torino 10129, Italy  
E-mail: [a.pedico@inrim.it](mailto:a.pedico@inrim.it)

A. Pedico, S. Bocchini  
Istituto Nazionale di Ricerca Metrologica  
Strada delle Cacce, 91, Torino 10135, Italy

A. Lamberti  
Center for Sustainable Future Technologies  
Istituto Italiano di Tecnologia  
Corso Trento, 21, Torino 10129, Italy

 The ORCID identification number(s) for the author(s) of this article can be found under <https://doi.org/10.1002/adsu.202400106>

© 2024 The Author(s). Advanced Sustainable Systems published by Wiley-VCH GmbH. This is an open access article under the terms of the [Creative Commons Attribution-NonCommercial](#) License, which permits use, distribution and reproduction in any medium, provided the original work is properly cited and is not used for commercial purposes.

DOI: 10.1002/adsu.202400106

Working on the spontaneous potential of the electrodes<sup>[6]</sup> and on the addition of a net surface charge on them,<sup>[7,8]</sup> the research pushed forward, showing the potential of this technique. Over the years, three different working principles have been investigated so far, namely, Capacitive Double Layer Expansion,<sup>[9]</sup> Capacitive Donnan Potential,<sup>[10–12]</sup> and Mixing Entropy Battery,<sup>[13,14]</sup> respectively based on the variation upon salinity change of the electric double layer capacity, on the Donnan membrane potential, and on the electrochemical energy of intercalated ions.

Various combinations of the working principles described above have been proposed in hybrid devices. In particular, the combination of ion exchange membranes (IEMs) with charged polymers (mainly polyelectrolytes) showed promising results. In 2016, Fernández et al. compared the CapMix performance using IEMs and charged polymers, suggesting that a combination of the two would outperform the singles and be beneficial to the process.<sup>[15]</sup> In 2020, Iglesias et al. proved that this idea could be successful, obtaining a device with improved energy extraction efficiency and cycle duration.<sup>[16]</sup>

In these kinds of devices, the IEMs are commonly based on polymers, since polymeric IEMs are the most diffused ones. Recently, graphene oxide (GO) has attracted the attention of the scientific community working on IEMs, mainly as an additive to boost the performance of IEMs.<sup>[17–19]</sup> However, in 2023, Aixalà-Perelló et al. demonstrated that also membranes made of pure GO can work efficiently as IEMs and that their selectivity can be tuned.<sup>[20]</sup> These results, combined with the versatility of GO and its ease of functionalization, pave the way for a wide range of potential applications, from the membrane and the energy storage fields, where GO is already known,<sup>[21,22]</sup> to new fields of application, like the energy harvesting from renewable sources.

In this context, this work investigates the possibility of using functionalized GO (fGO) and sulfonated poly(ether ether ketone) (SPEEK) coatings on activated carbon to obtain an asymmetric device suitable for CapMix application. The goal is to prove that also fGO can be efficiently used to boost the performance of devices used for CapMix, improving the stability of the system and increasing the extracted energy and power, which, to the best of our knowledge, has never been reported before. A thin film of positively charged fGO is deposited on the surface of an electrode made of activated carbon to create a thin layer of controlled charge on its surface. This fGO is obtained by grafting an acrylic monomer containing a quaternary amine group on the surface of GO. For the other electrode, the SPEEK is chosen as a counterpart of fGO. SPEEK is a polyelectrolyte renowned for its cationic exchange properties, commonly finding application in cation exchange membranes.<sup>[23–25]</sup> For this reason, the SPEEK is coated on the surface of the activated carbon, obtaining a negatively charged thin layer. The purpose of using the SPEEK is related not only to the possibility of increasing the stability of the electrode but also to providing negative voltage swings during CapMix cycles, a behavior of charged coating well-known in the literature.<sup>[26]</sup> The combination of these two materials is investigated here. Electrochemical characterizations have been used to investigate the electrochemical properties and to evaluate the feasibility of coupling these materials for CapMix application. After tuning the experimental parameters for the homemade setup, the results of the CapMix experiments show how an asymmetric cell assembled

with these electrodes can effectively harvest energy from salinity gradients with a stable output.

## 2. Experimental Section

### 2.1. Negative Charged Electrode Preparation

Poly(vinylidene fluoride) powder (PVDF,  $M_w$  534000, Merck) was dispersed in dimethyl sulfoxide (DMSO,  $\geq 99.5\%$  purity, Merck) in a concentration of 5 g L<sup>-1</sup> and then sonicated for 30 min using a frequency of 59 kHz in an ultrasonic bath (LBS2, FALC INSTRUMENTS SRL). Then, activated carbon power (AC, YP-50F, MTI Corporation) was slowly added. The slurry obtained in this way was then sonicated for 30 min and stirred overnight at room temperature. The final ratio (in weight) was 90% AC and 10% PVDF. No other solvents were added to the starting amount of DMSO. A variation of this preparation procedure had also been investigated, replacing the PVDF with the SPEEK to test the impact of different binders on the performance. The only difference in the preparation was the concentration of 40 g L<sup>-1</sup> in DMSO for the SPEEK, while the rest was kept the same. The synthesis of the SPEEK is described in a previous work.<sup>[27]</sup> Briefly, The SPEEK was prepared by dissolving 8 g of poly(ether ether ketone) ( $M_w$  20 800, Merck) in 50 mL of sulfuric acid (95–97% purity, Merck). After 96 h the solution was slowly added dropwise in a large excess of cold deionized water. After standing overnight, the precipitate was filtered and washed and thus dried at 60 °C in a vacuum oven.

A titanium foil (0.05 mm thickness, Goodfellow) was chemically and electrically insulated using a Kapton adhesive tape. Then, a window was cut on the insulation to expose a metallic area of 1 cm<sup>2</sup>. To obtain the electrode, the exposed titanium was coated with the slurry using the doctor blade method, exploiting a metallic cylinder with a spiral whose dimension allowed obtain a controlled thickness of the coated film  $\approx 150$   $\mu\text{m}$ . The electrode as prepared was dried at 60 °C for 15 min. The mass of the active material was roughly 5.5 mg cm<sup>-2</sup>.

After this step, half of the electrodes were coated with a thin layer of SPEEK, as described in previous work.<sup>[27]</sup> Briefly, the SPEEK was dispersed in DMSO at a concentration of 40 g L<sup>-1</sup>. An amount of 40  $\mu\text{L cm}^{-2}$  of this solution was drop-casted over the electrode surface. The electrode immediately underwent a drying step at 80 °C in low vacuum conditions for 1 h in a glass oven.

### 2.2. Positive Charged Electrode Preparation

GO flakes (Single layer GO, 300–800 nm of lateral dimension, Cheap Tubes Inc.) were functionalized following a two-step procedure described in previous work.<sup>[28]</sup> Briefly, GO flakes were dispersed in N,N-dimethylformamide (DMF,  $\geq 99\%$  purity, Merck) in a concentration of 1 g L<sup>-1</sup>. The dispersion was sonicated for 30 min at 40 kHz. Then, 4-hydroxybenzophenone (HBP, 98% purity, Merck) was added to the dispersion in an amount triple with respect to the mass of the GO. The dispersion obtained in this way was stirred and bubbled with N<sub>2</sub> for 30 min. At this point, it was exposed to UV radiation (UV solar simulator, Newport) for 5 min with an intensity of 200 mW cm<sup>-2</sup> while stirring. After this

treatment, the result was a reduced GO functionalized with the HBP. Subsequently, the dispersion was centrifuged (IEC CL10, Thermo Scientific) at 4000 rpm for 20 min. The precipitate was washed in ethanol (anhydrous,  $\geq 99.5\%$  purity, Carlo Erba) and centrifuged. This step was repeated three times to separate the unreacted material. The functionalized GO obtained in this way was dispersed again in DMF in a concentration of  $1 \text{ g L}^{-1}$ . To achieve the desired functionalization, the proper amount of (2-(acryloyloxy)ethyl)trimethylammonium chloride solution (80% in  $\text{H}_2\text{O}$ , Merck) was added to the dispersion in the ratio 5:1 with respect to functionalized GO. The solution was stirred, degassed by nitrogen bubbling, exposed to UV, centrifuged, and washed like before. The only difference was that the exposition time was 15 min in this case. After the final washing, the desired fGO was obtained and it was stored in ethanol at a concentration of  $5 \text{ g L}^{-1}$ .

Also, a second kind of functionalization was reported by Lyu et al.<sup>[29]</sup> has been investigated. Briefly, (3-chloropropyl)trimethoxysilane ( $\geq 97\%$ , Merck) and imidazole (99%, Merck) were mixed (molar ratio 1:1) for 24 h at  $110^\circ\text{C}$  under magnetic stirring in  $\text{N}_2$  atmosphere. The liquid obtained in this way was washed several times with ethyl acetate (99.8%, anhydrous, Merck) to remove unreacted products. GO flakes were dispersed in ethanol in a concentration of  $2 \text{ g L}^{-1}$  and sonicated for 30 min. Then, the two solutions were mixed for 4 h at  $50^\circ\text{C}$ . At the end of this step, a reduced GO functionalized with a monomer containing a positively charged imidazole group was obtained. This fGO was then filtered, washed several times with ethanol, and finally stored in ethanol at a concentration of  $5 \text{ g L}^{-1}$ . To distinguish between the two different materials, starting from here, the fGO obtained from UV grafting will be called fGO\_Am, while the other one will be called fGO\_Im. When not specified, fGO refers to both.

PVDF was dispersed in DMSO in a concentration of  $5 \text{ g L}^{-1}$  and sonicated for 30 min, like in the case of the negatively charged electrode. Then, the AC powder was slowly added and sonicated for 30 min. Finally, it was stirred overnight. As before, the final ratio of the slurry was 90% AC and 10% PVDF. No other solvents were added to the starting amount of ethanol and DMSO.

The positive electrode was obtained exposing a portion of a titanium foil covered with Kapton tape and then coating the slurry over it by doctor blade, followed by a drying step in oven, as previously described for the negative electrode. Then, the fGO dispersion was drop-casted over the active material surface with a loading of  $20 \mu\text{L cm}^{-2}$ . Finally, the solvent was dried under low vacuum conditions in a glass oven at  $80^\circ\text{C}$  for 1 h.

### 2.3. NaCl Solution Preparation

The sodium chloride (NaCl, anhydrous,  $\geq 99\%$  purity, Merck) was dissolved in deionized water (Direct-Q 3 UV, Merck Millipore) to obtain solutions of 600 and 10 mM for artificial seawater and freshwater, respectively.

### 2.4. Cell Design and Fabrication by Additive Manufacturing

The cell used for CapMix measurement is a homemade cell, comprising two round-shaped half-cells (Figure 1). The CapMix

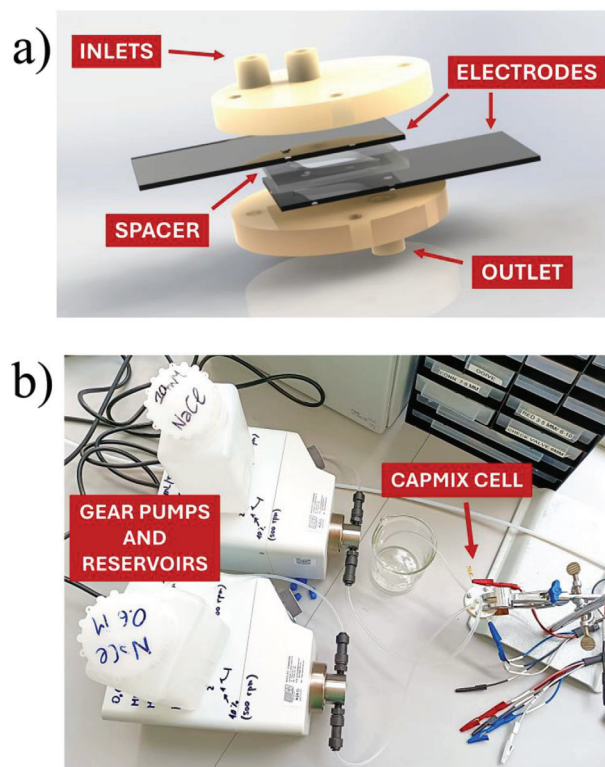


Figure 1. a) Expanded view of the CapMix cell. b) Experimental setup.

cell was designed in SolidWorks, according to the geometrical constraints and requirements. The material of the cell is the VeroWhite polymer by Stratasys. Such polymer is used as ink in the Objet30-Stratasys polyjet 3D printer. Once the CAD file containing information about the 3D geometry was sent to Objet30 3D printer, its software slices the volume, and the printheads deposit liquid VeroWhite resin, which was finally hardened by UV-lamp-induced polymerization. During the printing process, another resin was employed, namely the Support705 by Stratasys. This one was required to hang unsupported parts and allow the correct printing of the CapMix cell. After 3D printing, Support705 was mechanically removed by means of a waterjet process.

The diameter of the cell was 5 cm. A half-cell had two inlets, one for seawater and the other for freshwater. The other half-cell had only one outlet. The electrodes were placed in between, separated by a polymeric spacer made of transparent and chemically inert polydimethylsiloxane. The spacer acts as a fluidic chamber itself, thanks to its drop-like design optimized for water flow. The thickness of the spacer was 1 mm. The total volume of the fluid inside the cell (chamber + channels) was 0.15 mL. The area of the electrodes was  $1 \text{ cm}^2$ .

### 2.5. Characterization Techniques

Electron microscopy characterization was carried out with a Field-Emission Scanning Electron Microscope (FESEM Supra 40, manufactured by Zeiss) equipped with a Si(Li) detector (Oxford Instruments) for Energy-Dispersive X-ray (EDX) spectroscopy.

The electrochemical measurements were performed with a VMP3 potentiostat provided by Bio-Logic. This instrument offers a potential range of  $\pm 10$  V, a maximum current of 400 mA, with a resolution of 50  $\mu$ V and 760 pA. The accuracy was declared to be  $<0.1\%$  of the full-scale range. The electrometer had an input impedance greater than 1 T $\Omega$ , a capacitance of less than 20 pF, and a bias current lower than 5 pA.

## 2.6. Electrochemical Methods

Apart from the CapMix cycles, all the electrochemical characterizations were performed in a three-electrode configuration. The reference was an Ag/AgCl 3 M KCl electrode. The working electrode was produced as previously explained, while the counter electrode was prepared by mixing 85% wt. AC, 5% wt. carbon black (Timical C65, Imerys) and 10% wt. polytetrafluoroethylene (60% wt. dispersion in H<sub>2</sub>O, Merck) in ethanol. The slurry was dried until it got the consistency of a dough and then flattened over a titanium grid, resulting in a dense and thick layer. The layer was cut in the desired shape and dried at 60 °C overnight. This preparation resulted in a 1 mm thick stand-alone electrode.

Before any electrochemical characterization, the cell was rested at open circuit conditions for  $\approx 2$  h in seawater. The potentiostatic impedance spectroscopy was performed by applying a sinusoidal signal with an amplitude of 10 mV and a frequency ranging from 1 to 10 mHz. Cyclic voltammeteries were performed at a scan rate of 5 mV s<sup>-1</sup>, between 0 V vs open circuit potential (OCP) and  $\pm 1/-1$  V versus OCP, with steps of 100 mV. Anodic and cathodic scans were performed on different electrodes, to decouple the measurements. During each step, the cyclic voltammetry was repeated at least 50 times. All these measurements were performed in seawater solution, to be consistent with the CapMix tests.

For each material under investigation, the voltage rise as a function of the applied potential was evaluated. The adopted procedure included 5 min of constant voltage (from 0 V vs OCP up to the maximum of the potential window, with steps of 100 mV) in seawater, then some minutes in open circuit conditions, during which the seawater was replaced by freshwater. In this second step, the voltage rise was measured. When the potential reached a plateau, the freshwater was removed, and the seawater was poured in. The measurement was then repeated a total of five times to ensure reproducibility and check stability.

The CapMix was performed following the standard 4-steps CapMix cycle. A first step in which the cell was charged in high salinity solution, a second step in which the device was left in open circuit condition while the solution was switched to low salinity, then a discharge step, and finally another open circuit step in which the solution was switched back to high salinity. A gear pump (Analog Gear Pump, Masterflex) guarantees a constant and homogeneous water flux, providing a fast and smooth change of the whole volume of solution inside the CapMix cell. The charge and discharge steps were performed following two different strategies. The constant current (CC) and constant voltage (CV) methods were investigated. In both cases, the device was left 1 h in open circuit condition in a high salinity solution. After this time, the open circuit voltage (OCV) was set as the operating voltage at which the device was set to work, i.e., while cycling,

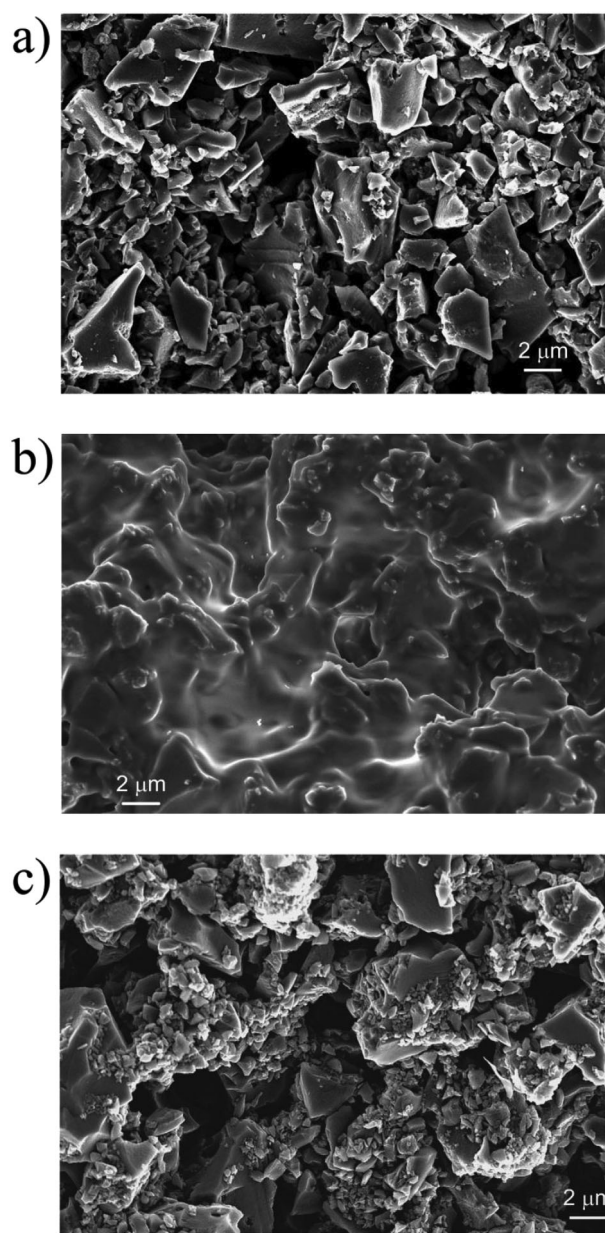


**Figure 2.** SEM images of the active materials: a) bare AC b) AC with SPEEK coating c) AC with fGO.

the cell was always charged and discharged up to that OCV value.

## 3. Results and Discussion

### 3.1. Material Characterization

Electron microscopy was employed to study the morphology of the as-prepared samples, and to check the uniformity of the active material. **Figure 2** reports a comparison of the active materials tested. The structure of the bare AC is reported in **Figure 2a**, where it is possible to appreciate the presence of micrometric particles. **Figure 2b** shows how the SPEEK coating is able to match

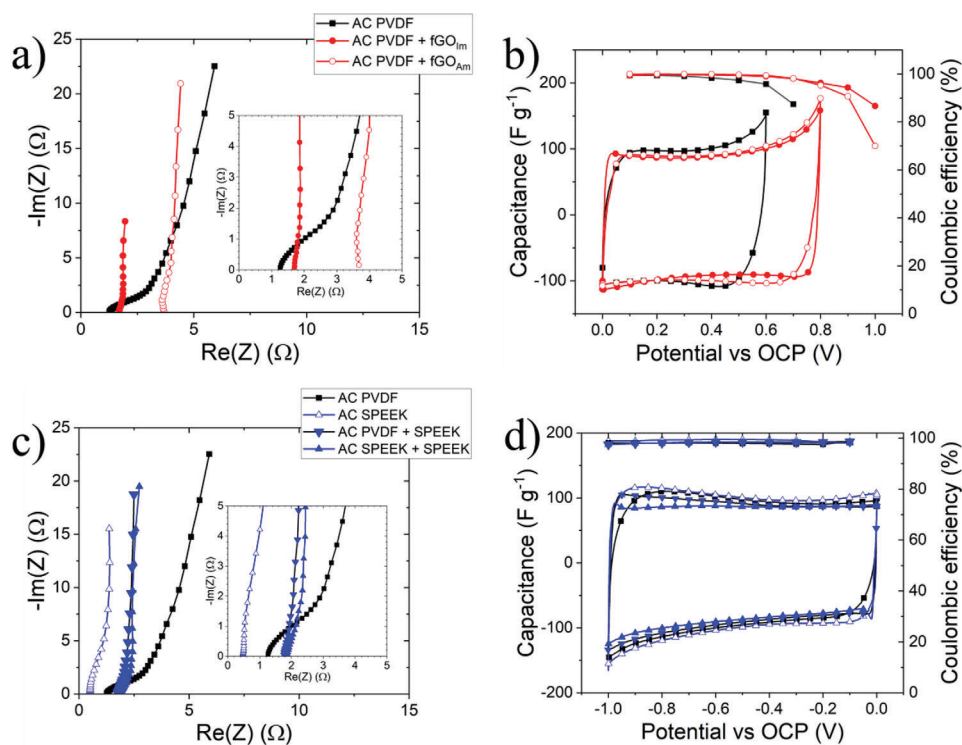


**Figure 3.** Electrochemical characterizations. a) Impedance spectroscopy on positive electrodes. b) Anodic scan of positive electrodes. c) Impedance spectroscopy on negative electrodes. d) Cathodic scan of negative electrodes.

the AC morphology, creating a uniform, thin, and continuous layer, while in Figure 2c it is possible to observe the presence of fGO flakes all over the AC substrate, even though this material was not able to create a uniform and continuous coating over the AC.

The electrochemical characterizations were implemented in order to evaluate the potentialities of the proposed electrodes for the CapMix application, investigating some key parameters such as capacitance, operative voltage windows, and equivalent series resistance. To do this, six different kinds of electrodes were studied:

- AC 90% wt. and PVDF 10% wt. (AC PVDF), both anodic and cathodic window;
- AC 90% wt. and PVDF 10% wt. with SPEEK coating (AC PVDF + SPEEK), cathodic window;
- AC 90% wt. and SPEEK 10% wt. (AC SPEEK), cathodic window
- AC 90% wt. and SPEEK 10% wt. with SPEEK coating (AC SPEEK + SPEEK), cathodic window;
- AC 90% wt. and PVDF 10% wt. with fGO<sub>Am</sub> coating (AC PVDF + fGO<sub>Am</sub>), anodic window;
- AC 90% wt. and PVDF 10% wt. with fGO<sub>Im</sub> coating (AC PVDF + fGO<sub>Im</sub>), anodic window;

Electrochemical impedance spectroscopy was initially performed on these electrodes, followed by cyclic voltammetry. The maximum operative voltage window was set by limiting the coulombic efficiency at than 95%.

For what concerns the anodic potential window, from Figure 3a it is possible to see how the introduction of fGO affected the equivalent series resistance (ESR), by increasing it. However, if Figure 3b is considered, the introduction of fGO provided an en-

largement of the operative voltage window of  $\approx 200$  mV, maintaining unaltered the overall capacitance of the electrode. Considering the cathodic potential window, it is possible to observe that the substitution of PVDF, as a binder of the electrode, with the SPEEK provided a reduction of the ESR. At the same time, if the SPEEK was used as an infiltrated ionic exchange membrane over the electrode, it increased the ESR. On the other hand, the SPEEK coating was not affecting the operative voltage window as well as the capacitance.

In order to select the optimal coupling between electrodes, the voltage rise was considered as a key parameter, since the potential difference between the electrodes during the switching of the solutions generates the voltage rise of the whole CapMix cell. Figure 4 reports the voltage rise of the different electrodes as a function of the applied voltage and the spontaneous potential.

From a direct comparison of Figure 4a,b, it is possible to note that the fGO-treated electrodes could produce a positive voltage swing even working at their spontaneous open circuit potential, while among the SPEEK-treated ones, only the AC SPEEK + SPEEK showed a negative voltage swing at its spontaneous potential. At negative potentials, the AC SPEEK + SPEEK is the best-performing electrode, while at positive potentials the behaviors of AC PVDF and AC PVDF + fGO<sub>Am</sub> are similar. However, maximizing the coulombic efficiencies and working as close as possible to the spontaneous potentials, the best choice is to couple the AC SPEEK + SPEEK and AC PVDF + fGO<sub>Am</sub> in a full device, with the aim of reducing as much as possible the losses while maximizing the voltage window and, therefore, the energy gain.

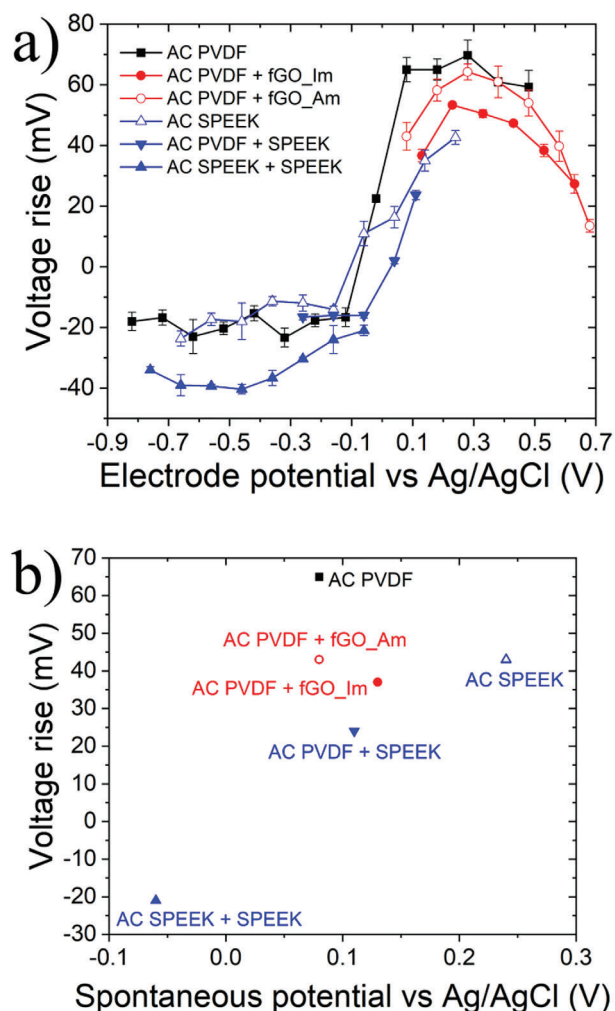


**Figure 4.** Voltage rise of different electrodes as a function of the: a) electrode potential b) spontaneous potential.

### 3.2. Capacitive Mixing

Initial tests were performed with a water flux of  $1 \text{ mL s}^{-1}$  and without limiting the time for each cycle, which means that the charge and discharge steps are manually triggered when reaching a plateau in the voltage. At this stage, the aim was to verify the correspondence between the data extracted from the electrochemical characterizations and the CapMix experiments.

The first results (Figure 5a) show that it is possible to obtain a constant behavior over time. The device spontaneously reached an OCV of 200 mV and then 50 cycles were performed, proving that it is possible to harvest a net amount of energy at each cycle. In this case, each cycle lasted 200–230 s for the CC method, 160–190 s for the CV method. The net energy gain comes from the difference between the energy extracted during the discharge step and the energy provided during the charge step. Energy is calculated as the integral over time of instant electrical power. Without optimization of the experimental parameters, the amount of harvested energy per cycle was  $0.31 \pm 0.03 \text{ J m}^{-2}$  for CC and  $1.37 \pm 0.12 \text{ J m}^{-2}$  for CV. The power output (evaluated

as the harvested energy from one cycle divided by the total time duration of the same cycle) was  $1.6 \pm 0.2 \text{ mW m}^{-2}$  for CC and  $8.0 \pm 0.8 \text{ mW m}^{-2}$  for CV. As expected, the power output is higher using the CV method rather than CC. In capacitive deionization, in which energy is provided to a supercapacitor to deionize water (i.e. the reverse process of CapMix), CC method is preferred to charge the electrodes because spikes of currents are avoided and, in general, is demonstrated that the energy consumption is lower.<sup>[30]</sup> Reversing the process, it becomes clear how using the CV method to extract energy provides a higher power output.

From this starting point, efforts were spent to boost the power output. The water flux was varied from  $0.5$  to  $5 \text{ mL s}^{-1}$  (Figure 5b). By balancing the trade-off between fast voltage rise and energy losses, the optimal value was set to  $1.5 \text{ mL s}^{-1}$ . Lower values badly affected the dynamics of the voltage rise, slowing the process and thus lowering the power output. Higher flux led to turbulent flux inside the cell which may directly affect the ions' distribution in the proximity of the electrodes, causing increased energy losses. A similar approach was followed for the duration of the cycle. Reducing the time spent to perform a cycle can boost the power output, however, it cannot be reduced indefinitely. The harvested energy is directly affected by the time duration of the charge and discharge steps. Therefore, a tradeoff between the time reduction and the power increase is intrinsically present. The optimal condition was found fixing the total duration of a cycle at 60 s. For the CC method, the duration of the charge step was set equal to 17 s, the OCV in low salinity equal to 18 s, the discharge step equal to 17 s, and the OCV in high salinity equal to 8 s (Figure 5c). In this case, the duration of the charge and discharge steps were kept the same since the current intensity was the same ( $0.1 \text{ A g}^{-1}$ ). For the CV method, the duration of the charge step was set equal to 10 s, the OCV in low salinity equal to 14 s, the discharge step equal to 20 s and the OCV in high salinity equal to 16 s (Figure 5d). Figure 5e shows the impact of optimization. Even though the total energy at stake was strongly reduced, the ratio between the harvested energy and the exchanged energy was increased, confirming the beneficial effect on the cycle. Figure 5f is a comparison of the power output, reaching up to  $6.4 \pm 0.7 \text{ mW m}^{-2}$  for CC and  $11.7 \pm 1.2 \text{ mW m}^{-2}$  for CV after optimization. Figure 5g is reported a graph showing the amount of exchanged energy (blue area), harvested energy (green area), and lost energy (red area) for each cycle, using the optimized parameters.

To provide an overview of the amount of free energy involved in the experiment, it is possible to evaluate the Gibbs free energy of mixing a NaCl 0.6 M solution with a NaCl 10 mM solution using the Pitzer equations for nonideal electrolytes, as described by Yip et al.<sup>[3]</sup> In this case, the energy at stake is  $\approx 0.23 \text{ kWh m}^{-3}$ , which represents the thermodynamic limit of the process, i.e., the maximum energy that can be extracted, theoretically. Considering the experimental conditions of this work, it translates into an energy of  $\approx 75 \text{ J}$  per cycle and a power of 1.25 W. As previously discussed, only a portion of this energy was used and even less was effectively harvested since the experimental conditions were optimized to maximize the power output of the materials, not to harvest the most energy out of it. However, these values indicate the possibility of harvesting much more energy increasing the area of the electrodes, while still being far from theoretical limits.

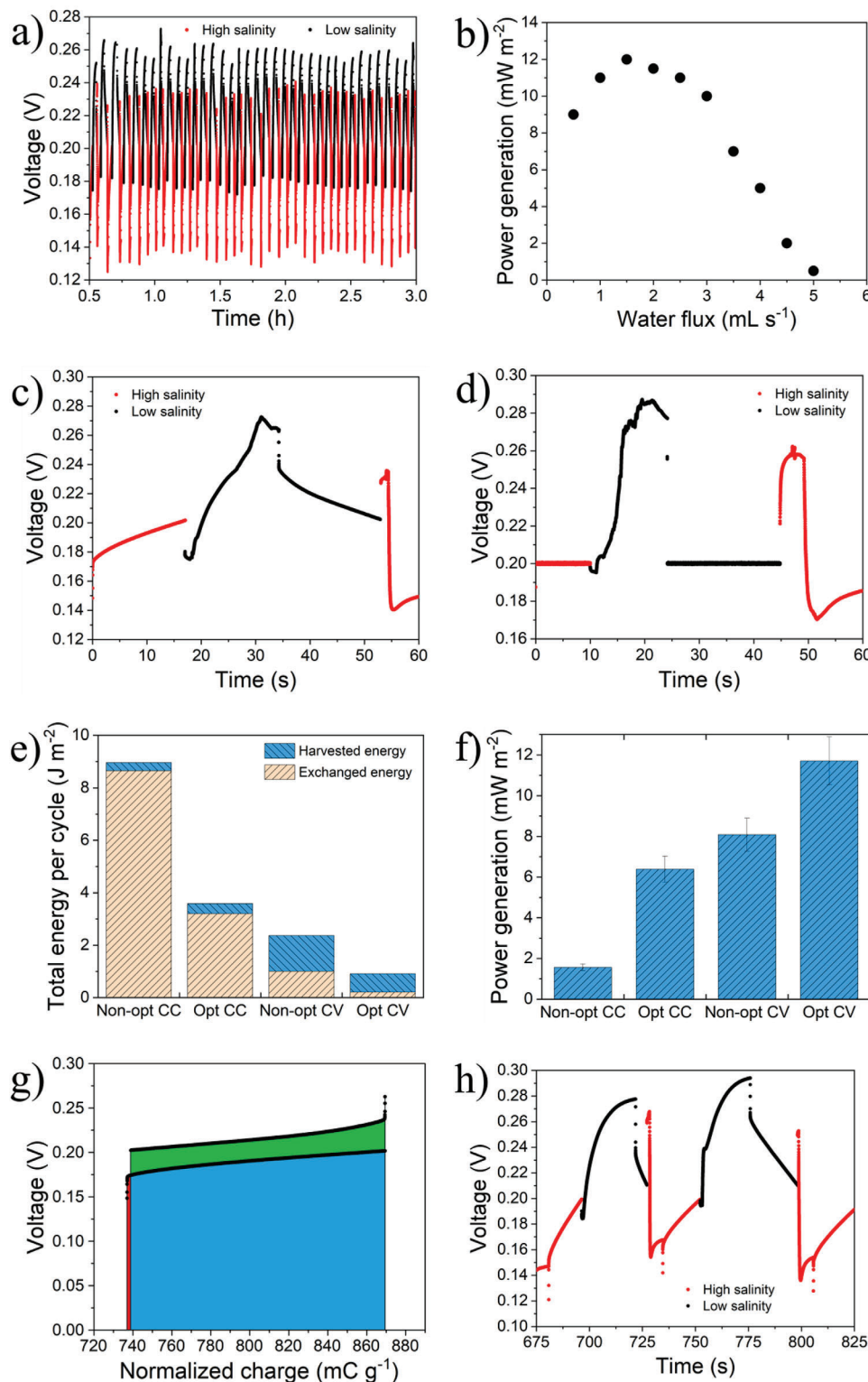


**Figure 5.** CapMix results. a) Example of CC method, not optimized. b) Power generation as a function of the water flux, using CV method. c) Optimized CC cycle. d) Optimized CV cycle. e) Comparison of exchanged and harvested energy in different conditions. f) Comparison of power output in different conditions. g) Charge and energy exchange in a CapMix cycle. The colored areas represent different energies: exchanged energy (blue), lost energy (red), and harvested energy (green). h) Example of cycles of AC SPEEK + SPEEK and AC PVDF, in which instability can be observed.



For the sake of comparison, CapMix experiments were performed also on a symmetric device whose electrodes were made of bare AC. With a starting OCV of  $\approx 1$  mV, the device was forced to work at 200 mV, following the same procedure used for the asymmetric device, allowing to direct comparison of the harvesting performance of the two devices. In the symmetric case, even if a voltage rise was observed when switching the solutions, both CC and CV methods were unable to harvest a net amount of energy over a cycle. This is because the extracted energy during the discharge step was lower compared to the energy provided to the system during the charge step. This was expected to happen, since the electrodes were forced to work far from their spontaneous potential, giving rise to intense phenomena of self-discharge, completely nullifying the contribution coming from the mixing energy.

Instead, an interesting result was obtained by combining AC SPEEK + SPEEK and AC PVDF. As expected, like in the case of AC PVDF + fGO\_Am, the OCV reached  $\approx 200$  mV. However, when performing CapMix experiments, an unstable behavior was observed (Figure 5h). Excluding the initial cycles which are usually required to reach a stable behavior, from one cycle to another, a huge variation in the amount of harvested energy was measured. While the voltage rise remained stable between 90 and 100 mV, the power output varied from  $0 \text{ mW m}^{-2}$  (no energy harvesting) up to  $10 \text{ mW m}^{-2}$ . Moreover, proceeding with the experiment, a negative trend in the power output was observed. Over time, the energy harvested at each cycle decreased, and the power output was reduced up to a maximum of  $1 \text{ mW m}^{-2}$  at the end of the experiment. These phenomena were addressed to poor stability over time of the positive electrode, which may shift its spontaneous potentials when cycling, giving rise to self-discharge phenomena. Indeed, after stopping the CapMix experiments, the OCV of the cell attested to  $< 130$  mV. The same thing did not happen with the AC PVDF + fGO\_Am, thanks to the presence of the net positive charge on the fGO which improved the stability of the system.

## 4. Conclusion

This study marks a significant milestone as it introduces, for the first time, the utilization of functionalized graphene oxide (fGO) in Capacitive Mixing (CapMix) experiments, demonstrating its effectiveness in harnessing energy from salinity gradients. The investigated device comprises two carbon-based electrodes, composed of activated carbon (AC) coated with fGO and sulfonated poly(ether ether ketone) (SPEEK) respectively. Comprehensive electrochemical characterizations have underscored the advantageous impact of the fGO coating on AC. The incorporation of fGO has notably elevated the device's performance, notably enhancing its stability over prolonged cycling. Following optimization of experimental parameters, the achieved power output stands at a remarkable  $12 \text{ mW m}^{-2}$ .

To further enhance the technology, future endeavors will concentrate on refining the uniformity of the fGO coating over the AC, with the ultimate goal of achieving the same level of uniformity observed with the SPEEK coating. The CapMix perspective will also drive ongoing research, focusing on refining the overall process, and cell design, and exploring novel materials. Additionally, there will be a dedicated exploration of the potential of fGO in

flowing-electrode CapMix configurations, aiming to propel performance to higher levels and achieve power output values in the range of tens or even hundreds of  $\text{mW m}^{-2}$ .<sup>[31,32]</sup> These advancements will not only contribute to the broader understanding of energy harvesting from salinity gradients but also hold promise for practical applications in sustainable energy systems.

## Acknowledgements

This result is part of a project that received co-funding from the European Research Council (ERC) under the European Union's ERC Starting Grant. Grant agreement "CO2CAP" No. 949916. This result is part of a project co-funded by the European Union – NextGenerationEU under the National Recovery and Resilience Plan (NRRP), Mission 04 Component 2 Investment 3.1 | Project Code: IR0000027 – CUP: B33C22000710006 – iENTRANCE@ENL: Infrastructure for Energy TRAnSition aNd Circular Economy @EuroNanoLab.

## Conflict of Interest

The authors declare no conflict of interest.

## Data Availability Statement

The data that support the findings of this study are available from the corresponding author upon reasonable request.

## Keywords

activated carbon, capacitive mixing, charged polymers, energy harvesting, graphene oxide

Received: February 9, 2024  
Revised: April 30, 2024  
Published online: May 29, 2024

- [1] S. E. Skilhagen, J. E. Dugstad, R. J. Aaberg, *Desalination*. **2008**, *220*, 476.
- [2] A. Cipollina, G. Micale, A. Tamburini, M. Tedesco, L. Gurreri, J. Veerman, S. Grasman, in *Sustainable Energy from Salinity Gradients*, Woodhead Publishing, Cambridge, UK **2016**, Ch5.
- [3] N. Y. Yip, D. Brogioli, H. Hamelers, K. Nijmeijer, *Environ. Sci. Technol.* **2016**, *50*, 12072.
- [4] D. Brogioli, R. Ziano, R. A. Rica, D. Salerno, F. Mantegazza, *J. Colloid Interface Sci.* **2013**, *407*, 457.
- [5] D. Brogioli, *Phys. Rev. Lett.* **2009**, *103*, 058501.
- [6] D. Brogioli, R. Ziano, R. A. Rica, D. Salerno, O. Kozynchenko, H. Hamelers, F. Mantegazza, *Energy Environ. Sci.* **2012**, *5*, 9870.
- [7] A. Siekierka, K. Smolińska-Kempisty, M. Bryjak, *Desalination*. **2020**, *495*, 114670.
- [8] M. C. Hatzell, M. Raju, V. J. Watson, A. G. Stack, A. C. van Duin, B. E. Logan, *Environ. Sci. Technol.* **2014**, *48*, 14041.
- [9] R. A. Rica, D. Brogioli, R. Ziano, D. Salerno, F. Mantegazza, *J. Phys. Chem. C*. **2021**, *116*, 16934.
- [10] O. Burheim, B. B. Sales, O. Schaeztle, F. Liu, H. V. Hamelers, *J. Energy Resour. Technol.* **2012**, *135*, 011610.
- [11] B. B. Sales, M. Saakes, J. W. Post, C. J. Buisman, P. M. Biesheuvel, H. V. Hamelers, *Environ. Sci. Technol.* **2010**, *44*, 5661.

- [12] K. Smolinska-Kempisty, A. Siekierka, M. Bryjak, *Desalination*. **2020**, 482, 114384.
- [13] F. L. Mantia, M. Pasta, H. D. Deshazer, B. E. Logan, Y. Cui, *Nano Lett.* **2011**, 11, 1810.
- [14] M. Ye, M. Pasta, X. Xie, Y. Cui, C. S. Criddle, *Energy Environ. Sci.* **2014**, 7, 2295.
- [15] M. M. Fernandez, R. M. Wagterveld, S. Ahualli, F. Liu, A. V. Delgado, *J. Power Sources*. **2016**, 302, 387.
- [16] G. R. Iglesias, S. Ahualli, A. V. Delgado, P. M. Arenas-Fernandez, M. M. Fernandez, *J. Power Sources*. **2020**, 453, 227840.
- [17] A. Alabi, L. Cseri, A. Al Hajaj, G. Szekely, P. Budd, L. Zou, *J. Membr. Sci.* **2020**, 594, 117457.
- [18] S. Gahlot, P. P. Sharma, H. Gupta, V. Kulshrestha, P. K. Jha, *RSC Adv.* **2014**, 47, 24662.
- [19] P. Kumar, S. Suhag, J. R. Mandal, V. K. Shahi, *Sep. Purif. Technol.* **2023**, 326, 124752.
- [20] A. Aixalà-Perello, A. Pedico, M. Laurenti, E. Fontananova, S. Bocchini, I. V. Ferrari, A. Lamberti, *NPJ 2D Mater. Appl.* **2023**, 7, 46.
- [21] A. Pedico, L. Baudino, A. Aixalà-Perello, A. Lamberti, *Membranes*. **2023**, 13, 429.
- [22] Y. Tian, Z. Yu, L. Cao, X. L. Zang, C. Sun, D.-W. Wang, *J. Energy Chem.* **2021**, 55, 323.
- [23] A. Rajput, S. K. Raj, J. Sharma, N. H. Rathod, P. D. Maru, V. Kulshrestha, *Colloids Surf. A*. **2021**, 614, 126157.
- [24] M. J. Parnian, F. Gashoul, S. Rowshanzamir, *Hydrogen Fuel Cell Energy Storage*. **2016**, 3, 221.
- [25] C. Zhao, H. Lin, K. Shao, X. Li, H. Ni, Z. Wang, H. Na, *J. Power Sources*. **2006**, 162, 1003.
- [26] M. Marino, L. Misuri, M. L. Jiménez, S. Ahualli, O. Kozynchenko, S. Tension, M. Bryjak, D. Brogioli, *J. Colloid Interface Sci.* **2014**, 436, 146.
- [27] D. Molino, A. Pedico, P. Zaccagnini, S. Bocchini, A. Lamberti, *Electrochim. Acta*. **2023**, 468, 143143.
- [28] A. Pedico, S. Bocchini, E. Tresso, A. Lamberti, *Adv. Mater. Technol.* **2022**, 7, 2101513.
- [29] Q. Lyu, H. Yan, L. Li, Z. Chen, H. Yao, Y. Nie, *Polymers*. **2017**, 9, 447.
- [30] Y. Qu, P. G. Campbell, L. Gu, J. M. Knipe, E. Dzenitis, J. G. Santiago, S. Michael, *Desalination*. **2016**, 400, 18.
- [31] Z. Zou, L. Liu, S. Meng, X. Bian, *Energy Rep.* **2022**, 8, 7325.
- [32] D. Kim, H. Kwon, G.-H. Cho, H. Kim, H. Seo, Y.-G. Jung, J. Choi, H. Kim, J. Yoo, D. Lee, I. Hwang, U. Paik, T. Song, H. Park, S. Yang, *Sep. Purif. Technol.* **2022**, 290, 120859.